Three-dimensional modelling of NOx and particulate traps using CFD: A porous medium approach

Benjamin, S.F. and Roberts, C.A.

Original citation & hyperlink:
Benjamin, S.F. and Roberts, C.A. (2007) Three-dimensional modelling of NOx and particulate traps using CFD: A porous medium approach. Applied Mathematical Modelling, volume 31 (11): 2446-2460.
http://dx.doi.org/10.1016/j.apm.2006.10.015

Three dimensional modelling of NOx and particulate traps using CFD: a porous medium approach

S. F. Benjamin and C. A. Roberts

Faculty of Engineering and Computing, Coventry University, Priory Street, Coventry CV1 5FB, UK

Abstract

Lean burn after treatment systems are the current focus for reducing emissions from diesel exhaust. The trend is for commercial CFD packages to use a single channel modelling approach. Due to computational demands, this necessitates specification of representative channels for modelling, implying prior knowledge of the flow field. This paper investigates a methodology for applying the porous medium approach to lean burn after treatment systems. This approach has proved successful for three way catalysis modelling and has the advantage that the flow field is predicted. Chemical kinetic rates for NOx trapping and regeneration in the model are based on information available in the open literature. Similarly, filtration information based on mass accumulation and soot combustion kinetics are also readily available. Modification of the source terms in a commercial CFD package enables prediction of trapping and release of NOx. This is an effective way to model a NOx trap after treatment system and provides simultaneous 3D modelling of the flow field. With diesel, particulate filtration is required. In the case of particulate traps, however, because of channel geometry, some assumptions are necessary for use of the porous medium approach and these are discussed in this paper. Both models produce qualitatively correct output and have parameters that can be tuned to conform to experimental data. Data to validate the NOx trap model is to be measured. The particulate trap model, on the other hand, is a feasibility study for modelling the complete diesel after treatment system using the porous medium approach.

Keywords: CFD model; porous medium; lean NOx trap; diesel particulate filter; emissions

1. Introduction

The popularity of diesel fuel has led to a focus on reduction of emissions from lean burn engines and the development of new after treatment systems. In such systems the main species of concern are NOx and particulates. As part of the development of these systems there is a need to model and predict the performance of the after-treatment components.

Automotive after-treatment catalyst bricks consist of multi-channel substrates or monoliths. The channels are often square in cross section, although monoliths with channels of other cross sectional shape are manufactured. The channel cross section dimension is about 1 mm. A thin layer of porous washcoat is applied to all channel walls and the active catalyst is embedded in the washcoat.

The lean NOx after-treatment system consists of two separate catalyst bricks, the diesel oxidation catalyst (DOC) and the lean NOx trap (LNT). The lean NOx after-treatment system functions by converting NO to NO_2 during lean operation, often on a Pt based DOC. The NO_2 is then stored in the LNT because the NO_2 reacts with a rare earth oxide such as BaO on the LNT to form a nitrate compound. The NOx is thus temporarily locked in the substrate. There is a finite amount that can be stored in the trap so after a period of time the trap is regenerated when the engine runs briefly rich, for a few seconds. The NO is released by breakdown of the nitrate under these conditions, and the released NO is reduced by the increased CO levels in the rich exhaust. Some authors consider that storage is as carbonate rather than nitrate but most kinetic schemes consider the formation and disintegration of nitrate.

Hepburn et al. [1] and Marshall et al. [2] published on 1D modelling and development of lean NOx after treatment systems, but for a gasoline engine. Their chemical scheme was complex. Their storage reaction considered NO_2 reacting with barium carbonate to form barium nitrate. Their regeneration scheme considered the reaction of the nitrate with both CO and hydrocarbon. Brogan et al. [3,4] also discussed such devices on gasoline engines but their work concentrated on NOx trap performance rather than on modelling. Wang et al.[5] (1999) reported a control oriented model of a lean NOx trap, but also aimed at GDI (gasoline direct injection) engines.

More recently, more complete kinetic schemes have been discussed in the literature. For example, Olsson et al. [6, 7, 8] describe a very comprehensive but also very complex scheme with multiple reactions. As the purpose of the present work is to develop a CFD model using the porous medium approach, a simpler scheme was required for development purposes. Laurent et al. [9] following on from Mahzoul et al.[10] describe such a scheme consisting essentially of just four reactions for NOx storage. The Laurent et al. scheme is capable of describing thermal trap regeneration, although not regeneration triggered solely by excess CO or hydrocarbon. Since most commercial CFD packages approach the chemistry of catalysis on the single channel basis, to avoid the excessive computational demands of full monolith modelling, this paper is an attempt to apply the porous medium approach [11] to NOx trapping. The porous medium approach can predict

simultaneously the flow field and the effect of chemical reactions on species conversion. The approach has been very successful on three-way catalysis [12, 13] and can be readily applied to NOx trapping systems.

Another element of the lean burn engine exhaust emissions strategy is the DPF (diesel particulate filter). This is more of a challenge for the porous medium approach. The channel geometry is more complex as the flow enters one channel and permeates to the neighbouring four channels through the monolith walls. Some significant assumptions must be made in order to model this device with the porous medium approach. This paper outlines a preliminary version of a model of a DPF filter as a porous medium and demonstrates that application of this approach could be feasible.

The commercial CFD package Star-CD Version 3.15 was used in the work described in this paper, but with amendments to the code made via user subroutines. This package was run either sequentially or in parallel on a 16 node Itanium2 64-bit cluster under HP-UX.

2. Theory

2.1 NOx trap model chemical kinetics scheme

To demonstrate the methodology of using the porous medium approach to model a NOx trap system, the simple chemical kinetic scheme of Laurent et al. [9] was chosen for NOx storage.

The formation of O*, NO* and NO2* occurs by reactions that are numbered 1 to 3 in the Laurent et al. paper[9]. The * symbol indicates that the radical is available on a Pt catalyst site or that a site is vacant. These are very fast reactions and are not considered to be rate determining re the formation and destruction of NO and NO_2. The main reactions considered by Laurent et al.[9] were as follows, with their numbering sequence retained:

$NO^* + O^* \rightarrow NO_2^* + *$	Rate 4, NO oxidation under lean conditions
$NO_2^* + * \rightarrow NO^* + O^*$	Rate –4, the reverse reaction
$BaO + 2NO_2^* + O^* \rightarrow Ba(NO_3)_2 + 3^*$	Rate 5, NOx trapping under lean conditions
$Ba(NO_3)_2 \rightarrow BaO + 2NO + 1.5O_2$	Rate 6, nitrate dissociation at high temperature

Laurent et al. [9] state the rates (mol/kg catalyst/s) for these reactions in the form of equations (1) to (5) below. They supply a complete set of numerical values for all of their kinetic rate constants, K_1 to K_3 and k_4 to k_6 .

$$r_4 = k_4 K_1 [X_{NO}] K_3^{0.5} [X_{O2}]^{0.5} / J^2 \quad (1)$$

$$r_{-4} = k_{-4} K_2 [X_{NO2}] / J^2 \quad (2)$$

$$r_5 = k_5 K_2 [X_{NO2}] K_3^{0.5} [X_{O2}]^{0.5} / J^2 \quad (3)$$

$$\text{Denominator term, } J = 1 + K_1 [X_{NO}] + K_2 [X_{NO2}] + K_3^{0.5} [X_{O2}]^{0.5} \quad (4)$$

$$r_6 = k_6 \psi^n_{nitr} = k_6 [f \psi_{nitr\,ref}]^n \quad (5)$$

The reference value $\psi_{nitr\,ref}$ can either be taken arbitrarily as unity or as the maximum permissible value for the catalyst, if that is known. The order of the reaction, n, is not specified in the paper by Laurent et al. but would be expected to lie between 0 and 1. It is taken as unity for the purposes of CFD model development.

Laurent et al. [9] state mass balances (mol/kg cat/s) for NO and NO_2 as follows:

$$\text{Net rate of NO production} = (r_{-4} - r_4 + 2 r_6) \quad (6)$$

$$\text{Net rate of } NO_2 \text{ production} = (r_4 - r_{-4} - 2 r_5) \quad (7)$$

$$\text{Net rate of } O_2 \text{ production} = (0.5 r_{-4} - 0.5 r_4 - 0.5 r_5 + 1.5 r_6) \quad (8)$$

$$\text{Rate of prodn. of } Ba(NO_3)_2 = (r_5 - r_6) \quad (9)$$

Use of these rate expressions enables source terms for chemical species to be specified in the CFD model.

2.2 NOx trap CFD methodology

Commercial CFD packages approach the chemistry of catalysis on the single channel basis. This makes heavy demands if full monolith modelling is attempted, with many thousands of computational cells required to describe each channel of a multi-channel monolith. Often, only representative channels are modelled to lessen the computational demand, but this requires prior knowledge of the detail of the flow field in order to select appropriate channels for study. Alternatively, it is possible to apply the porous medium approach, which can predict the flow field and the effect of chemical reactions on species conversion simultaneously.

For the porous medium approach the CFD model has a block of cells representing the fluid inlet. This is followed by the porous medium cells, which are used to model fluid flow through the catalyst monolith or monoliths. A final block of

cells models the fluid outlet. An extra block, or blocks, of cells with the same geometry as the porous medium cell block(s) represents the solid properties of the monolith(s) for heat transfer to the walls and conduction in the substrate. An example of a 3D mesh of this type is given in Fig 1 and will be discussed in more detail later. This porous medium approach to catalyst modelling is equally applicable to a simple 1D model made up of a single line of cells, or to a model having many cells and full 3D geometry. The mesh shown in Fig 1 could be modelled as an axisymmetric case, but many real systems are not axially symmetric, so this paper presents a simple 3D case as a demonstration of the methodology.

Full flow field predictions are possible with the porous medium approach because the resistance of the porous medium to flow is described by the expression

$$\frac{\Delta P}{L} = -\alpha U_s^2 - \beta U_s$$

where the permeability coefficient values α and β are assigned temperature dependent values that describe the behaviour of a catalyst monolith. High values of α and β preclude flow at right angles to the monolith axis. Upstream and downstream of the monolith the flow field is solved using the usual Reynolds averaged Navier Stokes methodology.

The modelling methodology requires that both the gas phase and solid phase species concentrations are properties of the porous fluid cells, since only the heat conduction equation with heat transfer source term is solved for the solid cells. The solutions for both the solid phase and gas phase concentrations are now obtained from the general conservation equation for chemical species, the transport equation, for which the full 3D version is shown below.

$$\frac{\partial \rho C}{\partial t} + \nabla \bullet (\rho U C) - \nabla \bullet \left[\left[\frac{\mu_t}{\sigma_s} + \rho D \right] \nabla C \right] = \text{Source } (kg/m^3/s) \qquad (10)$$

The four terms of this equation are referred to, from the left, as the transient term, the convective term, the diffusion flux term and the source term, the latter being applicable only within the porous fluid cells. The source term describes the net effect of diffusion of species between the gas stream and the washcoat at the channel wall as mass transfer and this replaces the diffusion flux term from gas to wall. This is achieved using a mass transfer coefficient derived from the thin film approximation. The diffusion flux along the channel length is assumed to be negligibly small compared with the convective flux.

Table 1 summarises what action is necessary to ensure that an appropriate equation is solved for either gas phase or solid phase species. The transient term is included in every case. Suppression of the diffusion flux term, which is present in

(10) above, is achieved by choice of appropriate values for parameters D and σ_s as indicated in Table 1. Thus, three different versions of the equation are solved, dependent upon the medium (fluid or porous) and the type of scalar species.

For the gas phase species in the porous medium, where the general diffusion flux term is suppressed, the transport equation for axial flow along the monolith is written as equation (11) below.

$$\frac{\partial}{\partial z}[\rho_{air}\, U_s\, C_g] + \varepsilon\, \rho_{air} \frac{\partial C_g}{\partial t} = \text{Source (kg/m}^3\text{ reactor/s)} \qquad (11)$$

Note that U_s is the superficial velocity for the porous medium such that

$$\rho_{air}\, U_s = \varepsilon\, \rho_{air}\, U \qquad (12)$$

Mass is generally transferred from the gas phase to the solid phase so that

$$\text{Source (kg/m}^3\text{ reactor/s)} = -K_{mi}\, \rho_{air}\, A_v\, [C_{i\,g} - C_{i\,sol}] \qquad (13)$$

A user subroutine provides the source terms for both gas and solid phase species to the CFD code. In the gas phase, mass transfer generally acts as a sink of species, as there is transfer to the washcoat pores due to the prevailing concentration gradient. For the solid phase species in the porous medium, the equation that describes the species transport is

$$V_w\, \rho_{air} \frac{\partial C_{i\,sol}}{\partial t} = K_{mi}\, \rho_{air}\, A_v\, [C_{i\,g} - C_{i\,sol}] + M\, R_i \qquad \text{kg/m}^3\text{ reactor/s} \qquad (14)$$

This states that mass is generally transferred from the gas phase to the solid phase and that reactions occur to species in the solid phase. The value for V_w in (14) used is 0.055 for development purposes, i.e. only about 1/20 of the reactor volume is available in the solid phase. This is derived from the assumption that the washcoat occupies about 11 % of the whole monolith reactor volume and the pores in the washcoat occupy about 50% of the washcoat volume.

Equation (14) can be re-expressed

$$\varepsilon\, \rho_{air} \frac{\partial C_{i\,sol}}{\partial t} = \{K_{mi}\, \rho_{air}\, A_v\, [C_{i\,g} - C_{i\,sol}] + M\, R_i\}\, [\varepsilon / V_w] \qquad (15)$$

Note that the form of equations (14) and (15) above is due to the modelling strategy of using a porous medium fluid computational cell to represent the gas contained in the washcoat pores, i.e. the solid phase. Equation (15) conforms to the required form of the transport equation for the CFD computation, which is shown in equation (16) below. Equation (16) has had both its general diffusion flux and convective terms suppressed, cf equation (10).

$$\varepsilon\, \rho_{air} \frac{\partial C_{sol}}{\partial t} = \text{Source (kg/m}^3\text{ reactor/s)} \qquad (16)$$

In the solid phase, in three way catalysts, mass transfer is a source of species whereas reactions generally consume the species, i.e. act as a sink. In the case of the NOx trap model, however, the situation is more complex as the reactions can both consume and create monitored species, dependent upon the air/fuel ratio, temperature etc. Hence R_i in equation (15) is the net reaction rate.

The values for M [kg /mol] are 0.030, 0.046 and 0.032 for NO, NO_2 and O_2 respectively. Thus the reaction terms in the source expressions for the three species in the solid phase for use in Star-CD are, from (6), (7) and (8):

Rate of NO reaction (kg NO /s /m^3 reactor) $$= \frac{0.030}{0.055} \varepsilon \rho_c (r_{-4} - r_4 + 2 r_6) \quad (17)$$

Rate of NO_2 reaction (kg NO_2 /s /m^3 reactor) $$= \frac{0.046}{0.055} \varepsilon \rho_c (r_4 - r_{-4} - 2 r_5) \quad (18)$$

Rate of O_2 reaction (kg O_2 /s /m^3 reactor) $$= \frac{0.032}{0.055} \varepsilon \rho_c (0.5 r_{-4} - 0.5 r_4 - 0.5 r_5 + 1.5 r_6) \quad (19)$$

The quantity ρ_c is catalyst loading. Laurent et al. [9] quoted a value of 818.4 kg /m^3 for their reactor tube experiment, but ρ_c has a much lower value numerically when the catalyst is applied as a washcoat to a substrate, as in an automotive exhaust NOx trap. Thus a value of about half of the Laurent et al. value has been used for model development purposes.

The net rate of production of nitrate in mol /kg cat /s is given by equation (9). The source expression for the nitrate can be re-expressed for use in the CFD model as follows:

$r_5 - r_6$ (mol nitrate /kg cat /s) $$= \psi_{nitr\ ref} \frac{\partial f}{\partial t} \quad (20)$$

Equation (20) can be re-expressed

$\varepsilon \rho_{air} \frac{\partial f}{\partial t}$ (kg /s /m^3 reactor) $$= [\varepsilon \rho_{air} (r_5 - r_6)] / \psi_{nitr\ ref} \quad (21)$$

The change from (20) to (21) is the same as made from (14) to (15) and this is discussed above. It enables the CFD programme to solve (21) for f, the value of the fraction.

Laurent et al.[9] imply that their model works well for excess O_2 (> 3%) but not well for less lean cases. Therefore, the scheme is switched off during regeneration periods. Reaction 6, with rate constant k elevated and adjusted is applied to release the stored NO during an appropriate time period. The released NO can be then be consumed by the NO/CO reduction reaction, for which kinetics are available in the paper by Siemund et al. [14]. The model has the facility that other

reaction equations with appropriate kinetics that consume NOx could be alternatively or simultaneously applied, if required.

Heat transfer in porous medium CFD models is managed in a similar way to mass transfer. Enthalpy exchange between porous medium (fluid) cells and solid cells is described by source terms and appropriate heat transfer coefficients. The heat conduction equation is solved in the solid cell blocks and an effective radial thermal conductivity describes heat conduction transversely across the monolith. If the axial thermal conductivity is significantly greater than the radial value, then this can be accounted for between adjacent cells in user subroutines by an additional source term.

2.3 Particulate trap model; methodology for applying equations to porous medium

A particulate trap or filter differs from a conventional catalyst substrate monolith in that alternate channels are blocked at inlet and at exit in a chequer-board pattern. The flow passes from an inlet channel to the neighbouring four channels through the channel walls, which are porous and perform the filtration.

For axial flow along the monolith the general equation (10) above can be written as

$$\frac{\partial \rho C}{\partial t} + \frac{\partial (\rho W C)}{\partial z} - \frac{\partial}{\partial z}\left[\left[\frac{\mu_t}{\sigma_s} + \rho D\right]\frac{\partial C}{\partial z}\right] = \text{Source (kg/m}^3\text{/s)} \qquad (22)$$

There are three main species of interest in the DPF model, namely soot in the gas phase, oxygen in the gas phase and soot that is lying in the layer on the filter surface. The latter is modelled as a gas phase species using a modified version of equation (22) that has only transient and source terms, cf equation (16) as described in the NOx trap model above.

The contents of the soot layer increases from approximately zero to a value that is large when expressed as a mass fraction of the fluid (gas). In order to solve the transport equation, a multiplier (10^4) can be introduced so that [true mass fraction $\times$ 10^{-4}] is solved for in the case of this scalar.

Regeneration occurs when temperature T rises. Equation (23) below, derived from simple geometry, can be used to estimate the soot layer thickness in a square channel.

$$w_p = \frac{1}{2}\left[a - \left(a^2 - \frac{M_p}{N_{cells} L \rho_p}\right)^{1/2}\right] \qquad (23)$$

The equation for a loaded filter as presented by Konstandopoulos et al. [15] is used to find the pressure drop across the filter

$$\Delta p = \frac{\mu Q (a + w_w)^2}{2 V_{trap}} \left[\frac{w_w}{k_o a} + \frac{1}{2 k_{soot}} \ln\left(\frac{a}{a - 2w_p} \right) + \frac{4 F L^2}{3 (a-2w_p)^4} + \frac{4 F L^2}{3 a^4} \right] \quad (24)$$

In applying this equation to a DPF monolith CFD model, Q is the global flow rate and μ is the local viscosity at the local cell temperature.

The flow in each inlet channel passes through the four walls into the four neighbouring outlet channels. Initially, filtration is assumed to be 100% efficient and uniform along the monolith length so that if there are 60 computational cells, then 1/60 of the mass available in the stream is "removed" and stored at each cell location. The amount of soot filtered is not calculated from the superficial axial velocity because velocity in the porous medium DPF model is the net or effective velocity through the whole substrate i.e. per inlet/outlet channel pair. Thus although the net velocity distribution across the whole monolith can be modelled in this way, the local mass flow rate is constant along the length of the substrate and hence is not directly related to the velocity through the filter wall at any particular axial location. The oxygen is assumed to react with the soot in the gas phase, however, because the stream flows through the soot layer in the real device. In the model, soot in the layer is accumulated by filtration and is removed by reaction. It should be possible to modify the model to account for an axial variation in thickness of the soot layer and its effect on the wall resistance and hence on local "through the wall" velocity and on the amount of soot subsequently deposited at each cell location.

Assume C1 is soot particulates expressed as a mass fraction of the gas, C2 is mass fraction of oxygen in the gas and C3 is soot fixed in the layer on the filter bed, but expressed as a mass fraction of the gas. The equations to be solved in the porous medium are

$$\varepsilon \rho_{air} \frac{\partial C1}{\partial t} + \frac{\partial(\rho_{air} W_s C1)}{\partial z} = \text{Sink of soot particulates by filtration (kg/s/m}^3\text{)} \quad (25)$$

$$\varepsilon \rho_{air} \frac{\partial C2}{\partial t} + \frac{\partial(\rho_{air} W_s C2)}{\partial z} = \text{Sink of } O_2 \text{ by reaction with soot in layer (kg/s/m}^3\text{)} \quad (26)$$

$$\varepsilon \rho_{air} \frac{\partial C3}{\partial t} = \text{Net effect (kg/s/m}^3\text{) of source by filtration and sink by reaction} \quad (27)$$

Note that W_s is the superficial velocity, $\varepsilon W_{channel}$.

Reaction rate constants attributed to Mogaka et al. are taken from the paper by Awara et al. [16] to determine the reaction rate by combustion of the soot layer. This is most significant during regeneration. Values for K_p of 3.68E+06 (/s) and for E_p of 142 (kJ/g mol) are used.

Particulate layer reaction rate (/s), $RR = K_p [O_2] \exp (- E_p / (R T))$ (28)

Regeneration occurs as soon as temperature rises sufficiently. The reaction is exothermic and the effect of the heat released on the solid substrate temperature is also accounted for in the model. The heat source for the solid cells is calculated in a user subroutine based on heat transfer between the gas phase and the solid phase, plus this additional term.

3. Results from the CFD models

3.1 NOx trapping and trap regeneration

Fig 1 shows a typical 3D mesh, having a total of 69920 cells. The 60 degree diffuser expands the flow from the 60 mm length inlet pipe to enter the oxidation catalyst, the first brick. There is a 12.7 mm gap between the bricks, then a NOx trap, and finally 38.1 mm of outlet duct. For parallel processing of the CFD model the mesh was partitioned manually by cell sets. It was partitioned into eight sets, with solid cells being kept together with their corresponding porous medium fluid cells. In order to achieve this the mesh blocks were sliced in half lengthways, to create hemi-cylinders. These were then sliced across. Thus the inlet pipe and diffuser made up two cell sets. The next two sets comprised the first brick, each set having both solid and fluid cells. The first part of the second brick also formed two sets and the final part of the second brick with the outlet duct made the final two sets.

Table 2 shows the inlet conditions for the simulation. The CO level was increased by a factor of 40 during the regeneration period and the oxygen level was decreased to approximate to rich engine exhaust conditions. The monolith diameter was 118 mm and the radial thermal diffusivity of the monolith was approximately 7.0E-07 $m^{2/}s$. The CFD simulations were run as transient using the PISO algorithm. The solver tolerances[17] were the default values of 0.01 for velocity and concentration, and 0.001 for pressure.

Fig 2 shows a cross section through the mesh shown in Fig 1. This is a typical CFD output contour plot showing the NO_2 level (mass fraction) after a period of several minutes of storage. The level can be seen to rise along the length in the first brick due to oxidation of NO to NO_2 and to fall in the second brick due to trapping of NO_2 by the reaction described as equation (3). The species concentrations are displayed only in the porous medium or fluid cells and not in the blocks that model the solid cells. Note the radial distribution of NO_2 in Fig. 2 ; this is caused by the non-uniform flow distribution at the front face of the oxidation catalyst. There is lower flow at the periphery and consequent higher conversion of NO to NO_2 because of increased residence time.

Fig 3 shows the cumulative NOx amounts at the CFD model inlet and outlet in a case where regeneration took place between 120 and 130 seconds. The amount of NOx is expressed in mol. of NOx supplied to 25 mm^2 of catalyst inlet face

area. Fig 3(a) shows a hypothetical case where regeneration occurs, but no consumption of species occurs by chemical reaction. Thus after the regeneration at 120 seconds the cumulative amount of NOx at exit rises to equal exactly what was supplied to the model at inlet. This demonstrates that the NOx trap regeneration and release part of the model is working correctly. Fig 3(b) shows the outcome when chemical reactions are included to consume the released NOx. Fig 3(b) shows one regeneration event only, but the reduction in emitted NOx would be significant over repeated storage and regeneration cycles. The regeneration rate can be controlled if necessary by adjustment of reaction rate constant k_6, see equation (5), during the regeneration period. It was found necessary to increase this by a factor of order 100 in order to promote completion of nitrate disintegration during the regeneration period. Similarly, the kinetics of the consumption reactions may need adjustment so that the level of NOx slip out of the monolith in Fig 3(b) matches experimental data correctly. Improved tuning will be attempted when data are available from an ongoing experimental programme[18].

Fig 4 shows nitrate levels during the regeneration in the same case as Fig 3(b). The measure of the amount of nitrate is a fraction of the reference level, which is 1.0 mol nitrate/kg catalyst mixture, see the definition of equation (5). The catalyst is assumed to be a formulaic blend of Pt, Barium compound and Al_2O_3. A value of 0.1 in Fig 4 corresponds to about half of the likely maximum possible storage in a trap of this type. The figure shows the nitrate stored at various locations, where Z 0.257 m represents the first cell of the computational model at the NOx trap inlet and Z 0.398 m is near the exit. It can be seen that the model predicts much higher levels of nitrate formation at the front of the brick with lower storage at the rear. Full regeneration can be seen to occur within about 5 seconds of the start of the regeneration. The species levels at input to the model are modified to a higher CO level and a lower oxygen level during the 10 second regeneration period.

3.2 Soot filtration in diesel particulate filter and filter regeneration by soot combustion

The mesh for the DPF simulation had 59280 cells. Figs 5, 6 and 7 show some results from that CFD model. The mass flow rate was 45 g/s to a 116 mm diameter substrate and the flow profile was uniform. A value of 2.6E-06 m2/s was used for the radial thermal diffusivity of the filter. The inlet soot mass fraction was 0.00021. The soot layer density was assumed to be 950 kg/m^3. The run was for 1800 seconds and regeneration was programmed to occur between 1050 and 1200 seconds. The inlet temperature was 450 K, except during the regeneration period when it was elevated to 850 K. The inlet mass fraction of oxygen was 0.035 throughout, i.e., the conditions were fuel lean. Fig 5 shows the build up of the uniform soot layer and the regeneration, with the soot layer reforming after the regeneration. Fig 5(a) shows a plot against time at three different locations in the DPF, whereas Fig 5(b) shows a plot against location at discrete times during the run. Fig 6 shows the detail of the regeneration. Fig 6(b) shows that the soot layer becomes non uniform during the regeneration. The soot combusts more readily near the front of the DPF. Fig 7 shows the monolith (solid phase) temperature predicted by the CFD model during the regeneration. The exotherm is seen to travel towards the rear of the

monolith as the regeneration proceeds. The exotherm subsides at the end of the regeneration period; all the soot is combusted without excessive temperatures being reached. This case allowed the soot layer to accumulate until it was equivalent to about 1% of the channel hydraulic diameter in thickness before regeneration was initiated.

Figs 8(a) and 8(b) show some results from a different CFD case. They show a cross section through a 3D DPF model with contour plots of the amount of soot present (expressed as mass fraction $\times 10^{-4}$) and temperature at a time instant during the regeneration. A higher level of soot per unit mass of air was input to this model and hence the mass fraction of the unconsumed soot in Fig 8(a) is 22 at the rear (cf between 12 and 14 in Fig 6). The mesh is similar to Fig 1 but there is only one brick, the DPF, which is 0.15 m in length. The soot level in Fig 8(a) is displayed on the porous medium cell block, not the solid phase cell block. This is because of the porous medium approach discussed in section 2.2 above, where the soot is treated as a species present in the gas phase. The temperature in Fig 8(b) is shown for both the solid cells, i.e. the substrate temperatures, and for the porous medium fluid cells, i.e. the gas temperatures. Fig 8(a) shows that the regeneration is localised at this time instant so that soot burn off has occurred notably in the front half of the DPF. The temperature plot shows a slightly higher solid phase temperature due to the exotherm. In Figs. 8(a) and 8(b) also note the radial distribution of soot and temperature that has been influenced by the maldistributed flow field at inlet to the diesel particulate filter.

4. Discussion of predicted results

The CFD run for the NOx trap 3D mesh on 8 processors took less than 8 hours to complete for 100 seconds of real time. The 3D DPF model took about 3 days on 8 processors but for the longer run of 1500 seconds of real time. These are fairly long computation times but at this stage optimising the efficiency of the computation has not been the main priority. With modifications aimed to improve and simplify the coding, more efficient mesh partition, strategic selection of parts of the run to be simulated, and choice of optimised time steps for transient runs it should be possible to reduce these computation times significantly.

The two models discussed above appear to produce qualitatively correct results. At this stage neither model is validated. A programme of experimental measurements on NOx trap performance is, however, underway at Coventry University. A test exhaust system is fitted downstream of a 2.0 litre diesel engine and high speed gas analysers are set up to monitor levels of CO, NO and NOx at inlet and exit during storage and regeneration. Catalyst substrate temperatures are also being monitored. Once this data is available it should be possible to tune the kinetics in the CFD model to match the experimental data. It is anticipated that the Laurent et al. model[9] will adequately describe the trapping during lean

operation, but it is known that this model is not appropriate under rich conditions. Modification of the constant k_6 in equation (5) is particularly important for modelling regeneration of the nitrate. The reactions and kinetics to be used to model NOx consumption during the regeneration period will also require investigation and verification.

The DPF model also performs well qualitatively. There are no plans currently, however, to validate this model, so the work reported here must be regarded solely as a feasibility study. The model clearly has the potential to predict effectively the performance of DPF systems. The current model could be improved by the inclusion of an algorithm to calculate the amount of soot filtered out in each computational cell at each time step dependent upon the existing soot layer thickness. This would be particularly important for cases where a non uniform soot layer of significant thickness remained at the end of the regeneration.

The main advantage of the porous medium approach is that it can predict the whole flow field in 3D cases. In the case of DPF filters, some are made from rectangular blocks of multiple channels that are cemented together during the manufacturing process to create the monolith. The cement layers behave as thick non-porous walls and distort the velocity profile distribution across the monolith, with very low velocities in the vicinity of the layers. Inclusion of these impermeable layers in a 3D mesh would enable the performance of a practical filter to be predicted, with due allowance for the significant maldistribution in velocity that is present in DPFs as currently produced.

The methodology of using the porous medium approach with suitable chemical kinetics to predict catalysis has been proven for three-way catalysis and it has been shown here that it can be applied to the newer technologies of NOx trapping and particulate filtration. The device of expressing solid phase species concentrations as quasi gas phase concentrations has been used successfully in both the NOX trap and the DPF models by modification of the source term expressions. Solution of modified versions of the transport equation with appropriate source terms has been described in this paper.

5. Conclusions

It has been demonstrated that the porous medium equivalent continuum approach can be successfully applied to modelling lean burn after treatment systems. The two systems investigated were the lean NOx trap and the diesel particulate filter. In both cases qualitatively correct output was obtained from 3D CFD models. The approach was applied by solving modified versions of the species transport equation. This was implemented by evaluating species source terms in the user subroutines of commercial CFD software. In the case of the NOx trap, both NOx storage and nitrate regeneration were described. In the case of the DPF, the soot layer build up by filtration was modelled and also the regeneration by soot combustion during the regeneration period. The porous medium approach has the advantage that when applied to a 3D

model it predicts full details of the flow field as well as the distribution of stored species and emissions. This is important in cases of flow maldistribution, notably current designs of DPF.

6. Acknowledgements

Technical and financial support from Jaguar-LandRover, ArvinMeritor and Johnson Matthey is gratefully acknowledged.

Nomenclature

a	channel dimension, side length if square cross section (m)
A_v	reactor surface per unit reactor volume (m^2/m^3)
C	mass fraction
C_g	species mass fraction in the gas phase
C_i	mass fraction of species i
C_{sol}	species mass fraction in the solid phase
D	species diffusivity (m^2 /s)
E_p	activation energy of thermal particulate oxidation reaction (kJ/kmol)
f	factor, fraction < 1
F	28.454 for square channels
k_i	reaction rate constant
k_o	specific permeability (m^2) of pristine channel wall
k_{soot}	specific permeability (m^2) of soot particulate layer
K_i	kinetic rate constant
K_{mi}	mass transfer coefficient (m/s)
K_p	frequency factor for oxidation of particulate matter (/s)
L	channel length, monolith length (m)
M	[kg /mol] for species i
M_p	accumulated mass of particulate matter or soot (kg)
N_{cells}	No. of cells containing soot
[O_2]	exhaust oxygen concentration, mole fraction (%)
Δp	pressure drop (Pa)
Q	volume flow rate (m^3/s)
R	gas constant, 8.314 (J /(mol K))
R_i	rate of production of species i by reaction (mol /s /m^3 reactor)

r_i	reaction rate for equation i
t	time (s)
T	temperature (K)
U	velocity in substrate channel (m/s)
U_s	superficial velocity for the porous medium, ε U (m/s)
V_{trap}	overall volume of monolith filter or trap (m^3)
V_w	volume in solid phase (pore volume) per unit volume of reactor [m^3 /m^3 reactor]
W	velocity component in the axial direction (m/s)
W_s	superficial velocity, $\varepsilon W_{channel}$ (m/s)
w_p	particle layer thickness that has accumulated on filter wall (m)
w_w	monolith wall thickness (m)
$[X_i]$	mol fraction of species i
z	axial coordinate
ε	porosity of the substrate expressed as a volume fraction
μ	viscosity (kg/(m s))
μ_t	turbulent dynamic viscosity (kg/(m s))
ρ	density (kg/m^3)
ρ_c	catalyst loading (kg cat /m^3 reactor)
ρ_p	density (kg/m^3) of layer of particulate matter or soot
σ_s	turbulent Schmidt No.
$\psi_{nitr\ ref}$	reference amount of Barium Nitrate (mol of nitrate/ kg cat.)

References

[1] Hepburn, J., Kenney, T., McKenzie, J., et al.

Engine and after treatment modelling for gasoline direct injection. SAE Paper No. 982596, 1998

[2] Marshall, R. A., Gregory, D., Eves, B., et al.

Optimising the after treatment configuration for NOx regeneration on a lean-NOx trap. SAE Paper No. 1999-01-3499.

Also published in GDI and Diesel After-treatment (1999) SAE SP-1476

[3] Brogan, M. S., Brisley, R. J., Moore, J. S., et al.

Evaluation of NOx adsorber catalysts systems to reduce emissions of lean running gasoline engines. SAE Paper No. 962045, 1996. Also published in SAE Transactions (1996) Vol. 105 pp 1916-1930

[4] Brogan, M. S., Clark, A. D., Brisley, R. J.

Recent progress in NOx trap technology. SAE Paper No. 980933, 1998. Also published in Catalyst Emission Control and Lean NOx Technologies (1998) SAE SP-1353

[5] Wang, Y., Raman, S., Grizzle, J. W.

Dynamic modelling of a lean NOx trap for lean burn engine control. Proceedings of the American Control Conference (1999) Vol. 2 pp 1208 –1212

[6] Olsson, L., Westerberg, B., Persson, H., et al.

A kinetic study of oxygen adsorption/desorption and NO oxidation overPt/Al_2O_3 catalysts. J Phys Chem B (1999) Vol. 103 pp 10433-10439

[7] Olsson, L., Persson, H., Fridell, E., et al.

A kinetic study of NO oxidation and NOx storage on Pt/Al_2O_3 and $Pt/BaO/Al_2O_3$. J Phys Chem B (2001) Vol. 105 pp 6895-6906

[8] Olsson, L., Fridell, E., Skoglundh, M., et al.

Mean field modelling of NOx storage on $Pt/BaO/Al_2O_3$. Catalysis Today (2002) Vol. 73 pp 263-270

[9] Laurent, F., Pope, C. J., Mahzoul, L., et al.

Modelling of NOx adsorption over NOx adsorbers. Chem Eng Sci (2003) Vol. 58 pp 1793-1803

[10] Mahzoul, H., Brilhac, J. F., Gilot, P.

Experimental and mechanistic study of NOx adsorption over NOx trap catalysts. Applied Catalysis B: Environmental (1999) Vol. 20 (1999) pp 47-55

[11] Benjamin, S. F., Roberts, C. A.

Modelling warm up of an automotive catalyst substrate using the equivalent continuum approach. Int J Vehicle Design (1999) Vol. 22 pp 253 – 273

[12] Benjamin, S. F., Roberts, C. A.

Automotive catalyst warm up to light off by pulsating engine exhaust. Int J Eng Res, (2004) Vol. 5 No. 2 pp 125 – 147

[13] Benjamin, S. F., Roberts, C. A.

Catalyst warm up to light off by pulsating engine exhaust: two-dimensional studies. Int J Eng Res (2004) Vol. 5 No. 3 pp 257 - 280

[14] Siemund, S., Leclerc, J. P., Schweich, D., et al.

Three way monolithic converter: simulations versus experiments. Chem Eng Sci , (1996) Vol. 51 No. 15 pp 3709 – 3720

[15] Konstandopoulos, A. G., Kostoglou, M., Skaperdas, et al.

Fundamental studies of diesel particulate filters: transient loading, regeneration and aging. SAE Paper No. 2000-01-1016. Also published in Diesel Exhaust After-treatment 2000 (2000) SAE SP-1497

[16] Awara, A. E., Opris, C. N., Johnson, J. H.

A theoretical and experimental study of the regeneration process in a silicon carbide particulate trap using a copper fuel additive. SAE Paper No. 970188, 1997. Also published in Diesel Exhaust After-treatment (1997) SAE SP-1227.

[17] Computational Dynamics.

Star-CD Users Guide and Methodology, Version 3.15, 2004

[18] Alimin, A. J., Roberts, C. A., Benjamin, S. F.

A NOx trap study using fast response emission analysers for model validation. SAE Paper No. 2006-01-0685, 2006. Also published in Diesel Exhaust Emission Control Modelling (2006) SAE SP-2023.

Tables

Table 1 Summary of modifications to species transport equation

	Gas phase scalars in fluid	Gas phase scalars in porous medium	Solid phase scalars in porous medium
Effective equation	(10)	(11)	(16)
Source term	Not included	Included	Included
Transient term	Included	Included	Included
Convective term	Included	Included	Not included
Diffusion flux term	Included	Suppressed	Suppressed
Diffusivity, D	Normal value, ~5.0E−05	1.0E−28	1.0E−28
Turb. Schmidt No., σ_s	Normal value	1.0E+28	1.0E+28

Table 2 Inlet conditions for NOx trap simulation

Parameter	Value
Flow rate (g/s)	47.5
Temperature (K)	650
NO mass fraction	0.000259
CO mass fraction	0.00058
NO_2 mass fraction	0.0000397
O_2 mass fraction	0.123

Abbreviated Title

Porous medium CFD model of NOx trap and DPF

Figure Captions

Fig. 1. Mesh for 3D NOx trap CFD model.

Fig. 2. Level of NO_2 shown as mass fraction during storage, prior to regeneration. Note that level increases in 1st brick (oxidation) and declines in 2nd brick (NOx is trapped). Species concentrations are displayed only in the fluid cell blocks.

Fig. 3. NOx trap model of regeneration showing (a) hypothetical case where released NOx is not consumed and (b) case where chemical reactions consume NOx released at regeneration.

Fig. 4. Regeneration of NOx trap showing nitrate levels at various locations from Z 0.257 m to Z 0.398 m in the NOx trap brick, where Z is measured from model inlet.

Fig. 5. DPF model output showing soot layer build up and regeneration in model development case with uniform filtration assumed; the same case is plotted in (a) as a function of time and in (b) as a function of location.

Fig. 6. DPF model output showing detail of soot layer regeneration in model development case with uniform filtration assumed; the same case is plotted in (a) as a function of time and in (b) as a function of location.

Fig. 7. DPF model showing monolith temperatures during regeneration triggered by an increase in temperature of exhaust gas; the same case is plotted in (a) as a function of time and in (b) as a function of location.

Fig. 8. (a) Amount of soot (mass fraction $\times 10^{-4}$) at an instant during regeneration. Soot level is shown in the fluid cells as a consequence of the porous medium methodology. (b) Temperature at the same time instant for gas and monolith shown separately in the respective cell blocks.

Benjamin and Roberts, Figure 1

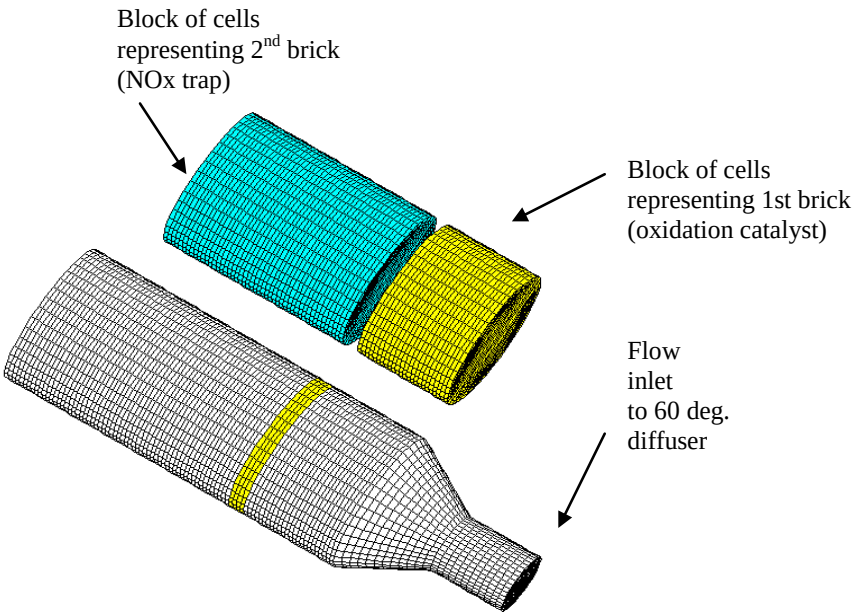

Benjamin and Roberts, Figure 2

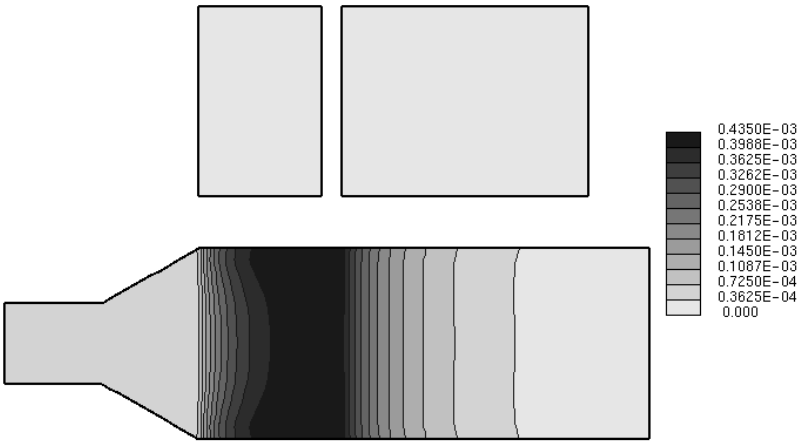

Benjamin and Roberts, Figure 3

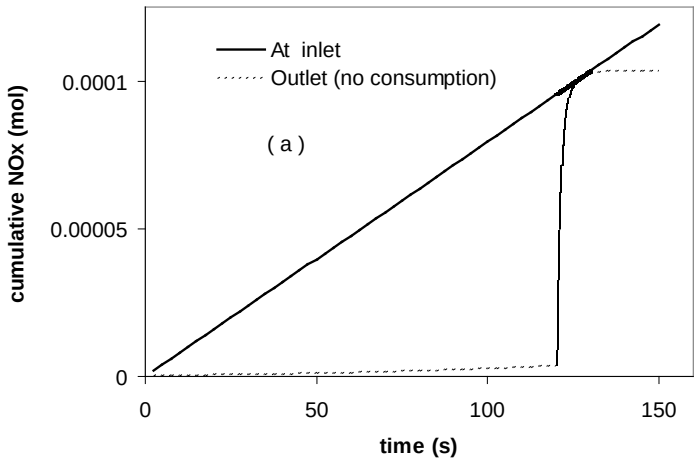

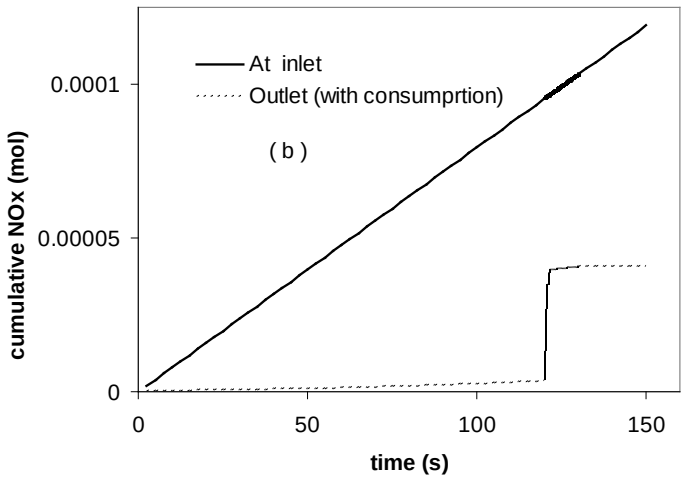

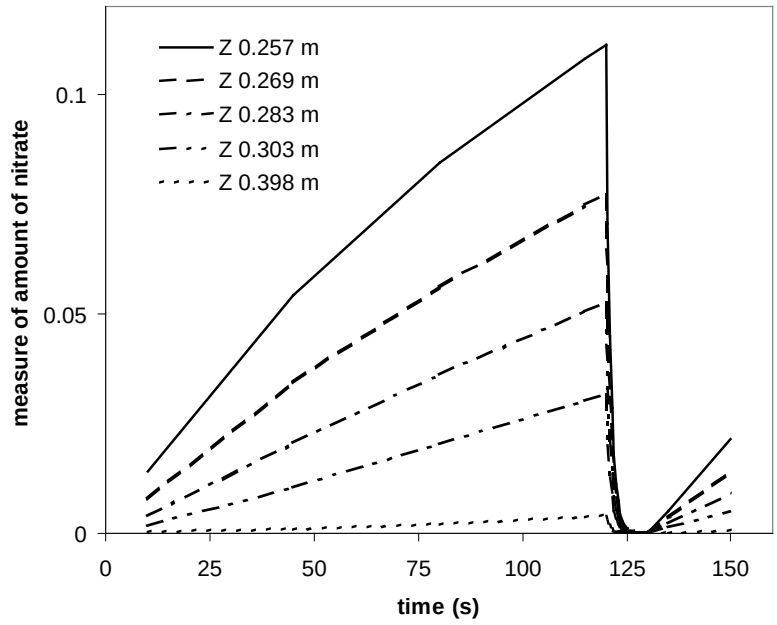
Z 0.257 m
Z 0.269 m
Z 0.283 m
Z 0.303 m
Z 0.398 m
measure of amount of nitrate
0.1
0.05
0
0
25
50
75
100
125
150
time (s)

Benjamin and Roberts, Figure 5

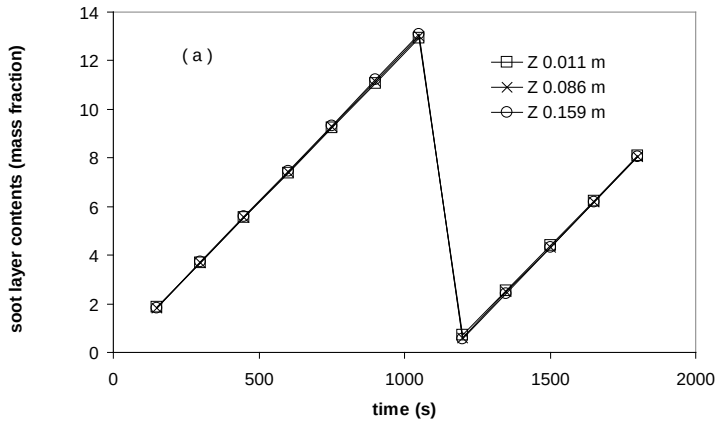

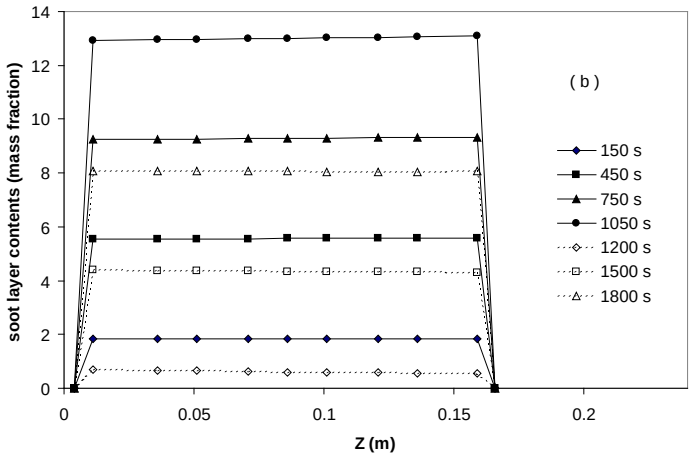

Benjamin and Roberts, Figure 6

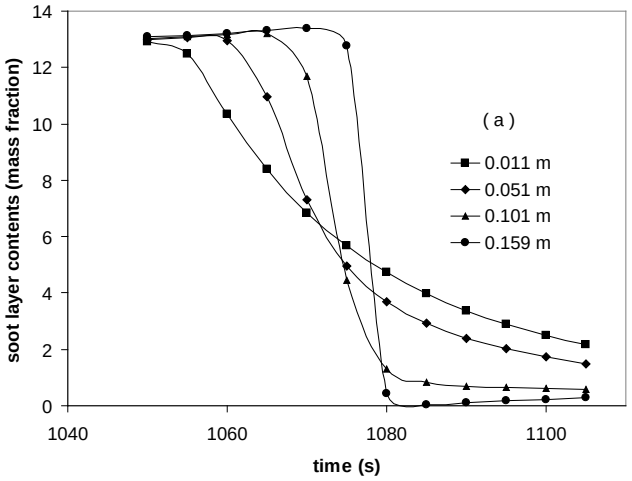

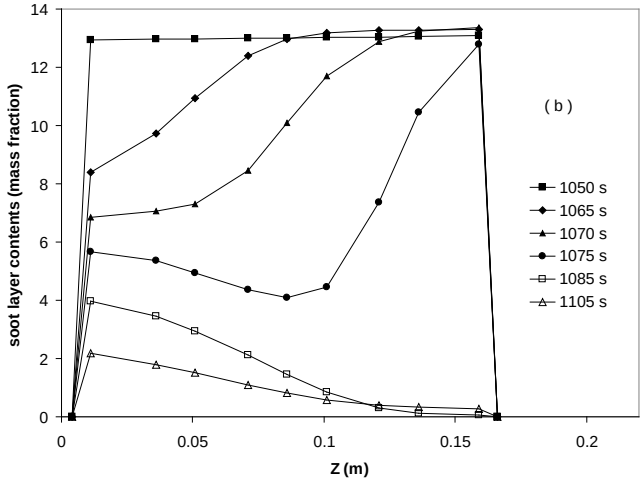

Benjamin and Roberts, Figure 7

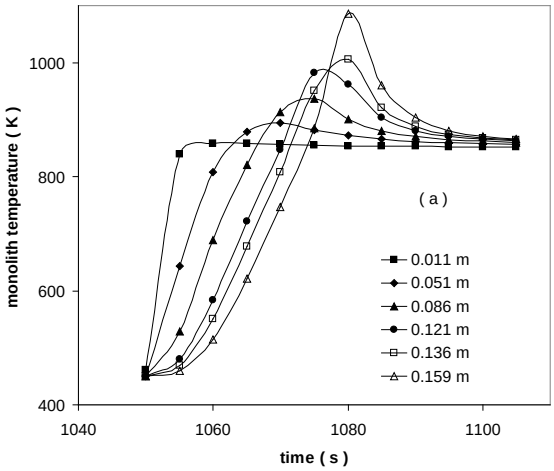

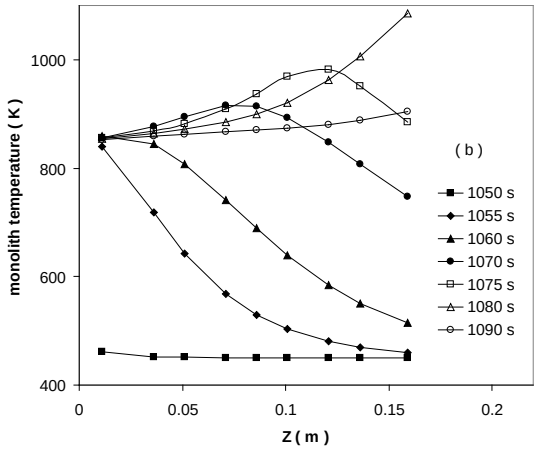

Benjamin and Roberts, Figure 8

(a)

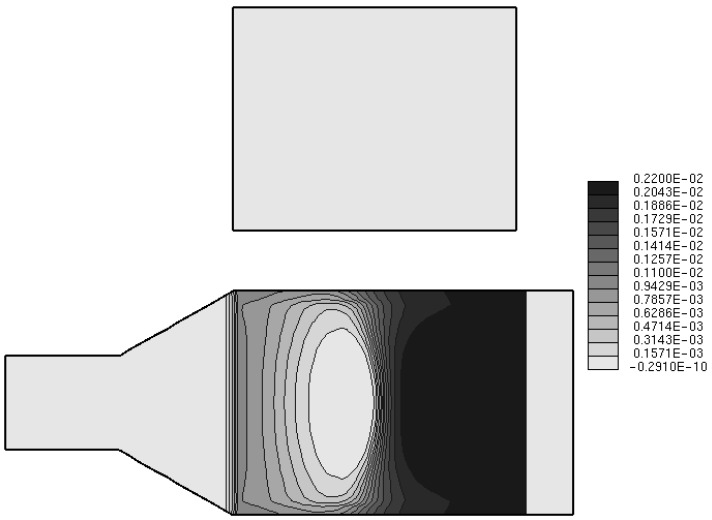

(b)